Dentomaxillofacial Radiology (2013) 42, 20120105

http://dmfr.birjournals.org

RESEARCH

Clinical evaluation of the normalized metal artefact reduction algorithm caused by dental fillings in CT

X-Y Gong*[,1], E Meyer[2], X-J Yu[1], J-H Sun[1], L-P Sheng[3], K-H Huang[1] and R-Z Wu[4]

[1]*Department of Radiology, Sir Run Run Shaw Hospital, Zhejiang University College of Medicine, Hangzhou, China;* [2]*Institute of Medical Physics, University of Erlangen–Nürnberg, Erlangen, Germany;* [3]*Dental Department, Sir Run Run Shaw Hospital, Zhejiang University College of Medicine, Hangzhou, China;* [4]*Siemens Healthcare China, Beijing, China*

Objectives: The aim of this study was to evaluate the performance of a normalized metal artefact reduction (NMAR) algorithm in patients with high-density dental fillings in CT images, and compare the results with weighted filtered back-projection (WFBP) and linear interpolation metal artefact reduction (MARli) algorithms.

Methods: A total of 15 patients who had dental fillings were included in this study. The CT raw data sets were processed on an offline workstation. For each data set, one image series was reconstructed with WFBP, one with MARli and one with NMAR. Two observers qualitatively graded the severity of metal artefacts and their impacts on surrounding and distant soft tissue using a five-point scale. Six regions of interest were selected to measure the CT values and the standard deviation (SD) for quantitatively evaluating the effects of artefact reduction.

Results: A total of 217 slices with metal artefacts from 15 patients were included in the qualitative analysis. The average score (mean ± SD) with the WFBP and MARli algorithms was 2.24 ± 1.06 and 2.71 ± 0.73, respectively. Image artefacts were significantly reduced using the NMAR algorithm compared with the other two algorithms, with an average score of 1.70 ± 0.83. The mean CT value in the most hypodense streak artefacts around the metal fillings was significantly improved with both MARli and NMAR. The mean SDs of measured CT values from surrounding or distant soft tissues were lower in NMAR images than in WFBP and MARli images.

Conclusions: The NMAR algorithm can significantly reduce the artefacts caused by dental fillings, compared with the WFBP and linear interpolation algorithms.

Dentomaxillofacial Radiology (2013) **42,** 20120105. doi: 10.1259/dmfr.20120105

Cite this article as: Gong X-Y, Meyer E, Yu X-J, Sun J-H, Sheng L-P, Huang K-H, et al. Clinical evaluation of the normalized metal artefact reduction algorithm caused by dental fillings in CT. *Dentomaxillofac Radiol* 2013; **42:** 20120105.

Keywords: dental filling; metal artefact reduction; CT; X-ray; normalized metal artefact reduction

Introduction

Metal implants, such as dental fillings, hip prostheses, implanted marker bins, surgical clips, cardiac pacing devices and brachytherapy seeds, are not uncommon in patients undergoing CT examinations.[1–4] These metallic implants can produce severe image artefacts in the form of streaks or dark shadows. The artefacts not only lead to insufficient image quality for diagnosis but also make it difficult to delineate anatomical structures which are important for image-guided intervention procedures.[4,5] Moreover, these artefacts may disallow tumour and organ delineation and compromise dose calculation outcomes in radiotherapy.[6,7]

The metal artefact remains the main limitation of applying CT in the craniofacial area in patients with dental fillings. Dental fillings or dental implants usually use high-density metal materials, such as gold alloy, amalgam and co-chrome, which cause severe artefacts

*Correspondence to: Dr Xiang-yang Gong, Department of Radiology, Sir Run Run Shaw Hospital, Zhejiang University College of Medicine, 3 East Qingchun Road, Hangzhou 310016, China. E-mail: cjr.gxy@hotmail.com
Received 16 March 2012; revised 25 July 2012; accepted 26 July 2012

and frequently obscure observation of the anatomy and lesions in the maxilla, mandible, nearby tooth, tongue, para-oropharynx and neck soft tissues, and sometimes the cervical vertebral, cervical spine and paravertebral structures. However, patients are not always able to remove all metal materials from their teeth when they undergo CT examination. So far, metal artefacts have been the main drawback of detecting lesions in the craniofacial area in clinical situations.

Increasing the tube current may reduce the noise in the projection data but does not correct for other data inconsistencies caused by metal implants.[8] The use of a higher kilovolt peak may improve the image quality because of the greater penetrating capability of the high-energy photons and lower beam hardening effect.[9] However, the radiation dose that the patient receives is increased. High-energy reconstructions with dual energy CT data sets can significantly reduce metal artefacts and improve image quality and diagnostic value.[10] However, dual energy CT is not sufficiently effective for dental fillings. Some novel methods have been introduced to remove the metal artefacts from dental fillings. Nakae et al[11] used gantry tilt scanning as an image reconstruction technique to improve image quality and remove most artefacts caused by metallic dental fillings. The resulting images could be used in the evaluation of oropharyngeal lesions in patients with dental fillings. Park et al[12] used additional silicone dental impression materials as a "tooth shield" for the reduction of metal artefact caused by metal restorations and orthodontic appliances.

The metal artefact reduction (MAR) algorithms based on interpolation can also be useful for MAR. These methods have problems such as loss of detail around the metal–tissue interface, and they sometimes introduce new artefacts to the images.[10] Meyer and colleagues[13] introduced a novel normalized metal artefact reduction (NMAR) technique that generalizes the idea of an MAR algorithm based on simple length normalization. NMAR outperformed filtered back-projection, the linear interpolation MAR algorithm and the algorithm based on simple length normalization in artefact reduction for both moderate and severe artefacts. They proposed that NMAR could be used as an additional step in any conventional sinogram inpainting-based MAR method.[13] In this study, we evaluated the performance of the NMAR algorithm in patients with high-density dental filling artefacts and compared it with weighted filtered back-projection (WFBP) and MAR based on a linear interpolation MAR algorithm (MARli).

Materials and methods

Patients

A total of 15 patients (5 male, 10 female) with a mean age of 45.3 years (age range 24–67 years) who had dental fillings were included in this study. Dental filling materials included amalgam ($n = 7$), co-chrome ($n = 4$), nickel–chrome ($n = 3$) and gold alloy ($n = 1$).

CT scan

All CT examinations were performed with a 20-detector-row multislice spiral CT scanner (Somatom Definition AS; Siemens, Forchheim, Germany). Scan parameters were: tube voltage, 120 kVp; tube current–time, 72 mAs; collimation, 20×0.6 mm; pitch, 0.8; gantry rotation time, 0.5 s.

CT data reconstruction

The CT raw data sets were exported to a DVD and processed on an offline workstation equipped with the software tools for image reconstruction.[13–15] For each data set, one image series was reconstructed with WFBP, one with MARli and one with NMAR. All images were reconstructed with a slice thickness of 1 mm, an increment of 1 mm, a medium soft kernel of H10 and a field of view of 250 mm.

Weighted filtered back-projection: The images were reconstructed with the WFBP algorithm from Stierstorfer et al.[14] This is an approximate filtered back-projection-type reconstruction algorithm for dedicated use with multislice spiral CT of arbitrary pitch.

Metal artefact reduction with linear interpolation: A simple approach to correct metal artefacts with MARli has been described previously.[15] The purpose of this algorithm is to replace the metal-affected parts of the raw data, which are often called the metal trace or metal shadow. As the first step, the metal trace has to be determined. In order to do this, an uncorrected image is reconstructed with WFBP. From this image, a metal mask image is segmented. Then, the metal mask is forward-projected to obtain artificial raw data. The positive entries in these raw data of the metal mask define the location of the metal trace. The next step is to replace this part in the original raw data by linear interpolation. These modified raw data are reconstructed by WFBP again. To visualize the metal implants, the metal image, which was segmented from the uncorrected image at the beginning, is reinserted into the MARli image.

Normalized metal artefact reduction: The NMAR algorithm was described by Meyer et al.[13] Briefly, for the NMAR algorithm, an image has to be reconstructed which is pre-corrected by MARli as described in the subsection above. Subsequently, a prior image is computed from this image. In this prior image, all pixels below a threshold of -500 HU are regarded as air regions and are set to -1000 HU. Pixels between this threshold and a threshold for bone are set to 0 HU. Bone pixels remain unchanged.

In the next step, artificial raw data of the prior image are obtained by forward-projection. Subsequently, the original raw data are normalized by dividing them pixel-wise by the raw data of the prior image. The metal

trace in this normalized data set is then replaced by linear interpolation.

After interpolation, the data set is denormalized by multiplying it pixel-wise with the raw data of the prior image. By this step, information about the structures which are contained in the prior image is brought back into the metal trace. These corrected raw data are finally reconstructed by WFBP. To visualize the metal implants, the metal image, which was segmented from the uncorrected image at the beginning, is reinserted into the NMAR image.

Image evaluations

Two readers qualitatively graded the severity of metal artefacts and their impacts on surrounding and distant soft tissue together with discussion using a five-point scale. A score of 0 indicated the absence of artefacts and that the surrounding tissues were fully assessable. A score of 1 indicated minor streak artefacts, but that the structures around the metal implants were distinguishable. A score of 2 represented pronounced streaks, and that the structures around the metal implants were indistinguishable but the distant soft tissues (cervical spine, vertebral, neck muscles etc.) were clear. A score of 3 indicated severe streaks, and that the observation of distant soft tissue was obscured. A score of 4 represented massive artefacts and that the CT image had no diagnostic value.[10] Evaluation of the image was performed on a medical monitor. The CT image of the same slice but reconstructed with different algorithms was simultaneously shown on soft-tissue window settings (width 400 HU, centre 40 HU). Slices free of metal artefacts on any of the three reconstructed images of the same slice were omitted for the evaluation.

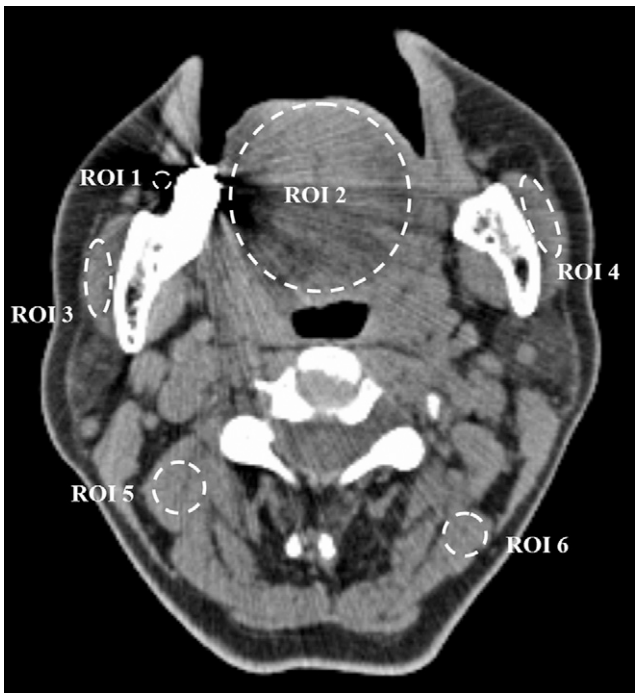

Figure 1 Example image showing the regions of interest (ROIs) for quantitative measurement

For quantitative evaluation, six regions of interest (ROIs) on each CT image were selected and measured (Figure 1). The ROIs included were as follows: the ROI covering the darkest area of the streak artefacts (ROI_1); the ROI covering the tongue as much as possible (ROI_2); the ROIs covering the right masseter muscle (ROI_3) and the left masseter muscle (ROI_4) as much as possible; and the ROIs covering the muscles in the right (ROI_5) and left (ROI_6) posterior cervical regions avoiding fat. The location and size of each ROI changed according to the changing of anatomical structures slice by slice. However, all six ROIs were identical for three images within the same slice set. The same observer defined the ROIs and measured the mean CT values and standard deviation (SD) for each ROI.

Statistical analyses

All statistical analysis was performed with a commercial statistical software package (SPSS® 17.0 for Windows; SPSS Inc., Chicago, IL). A repeated measure analysis of variance was used for the image score and quantitative evaluation. A p-value of 0.05 was defined as statistically significant.

Results

Qualitative evaluation

A total of 217 sets of slices with artefacts from 15 patients were included in the qualitative analysis. The average artefact score (mean ± SD) with WFBP and MARli was 2.24 ± 1.06 and 2.71 ± 0.73, respectively. With the MARli algorithm, artefacts were reduced in only a few images. In the majority of images, the artefacts were equal to or worse than the WFBP reconstruction images. Image deterioration appeared as streak widening, streak shifting and generation of new artefacts (Figure 2). With the NMAR algorithm, metal artefacts were significantly reduced and image quality was improved compared with WFBP and MARli, with an average score of 1.70 ± 0.83 (Figure 3). There were significant differences ($p < 0.001$) among the average scores of the three reconstruction methods.

Quantitative evaluations

The mean CT value in the most pronounced hypodense streak artefacts around the metal implants was −374.59 ± 277.72 HU in the 217 slices with the WFBP algorithm, which was significantly improved with either MARli (−263.38 ± 96.34 HU) or NMAR reconstruction (−282.02 ± 152.30 HU) with $p < 0.001$.

The mean CT values from ROI_2 to ROI_6 had no statistically significant differences among the three groups of images (Table 1).

A small SD of the CT values indicates a homogeneous intensity distribution in the respective ROI.

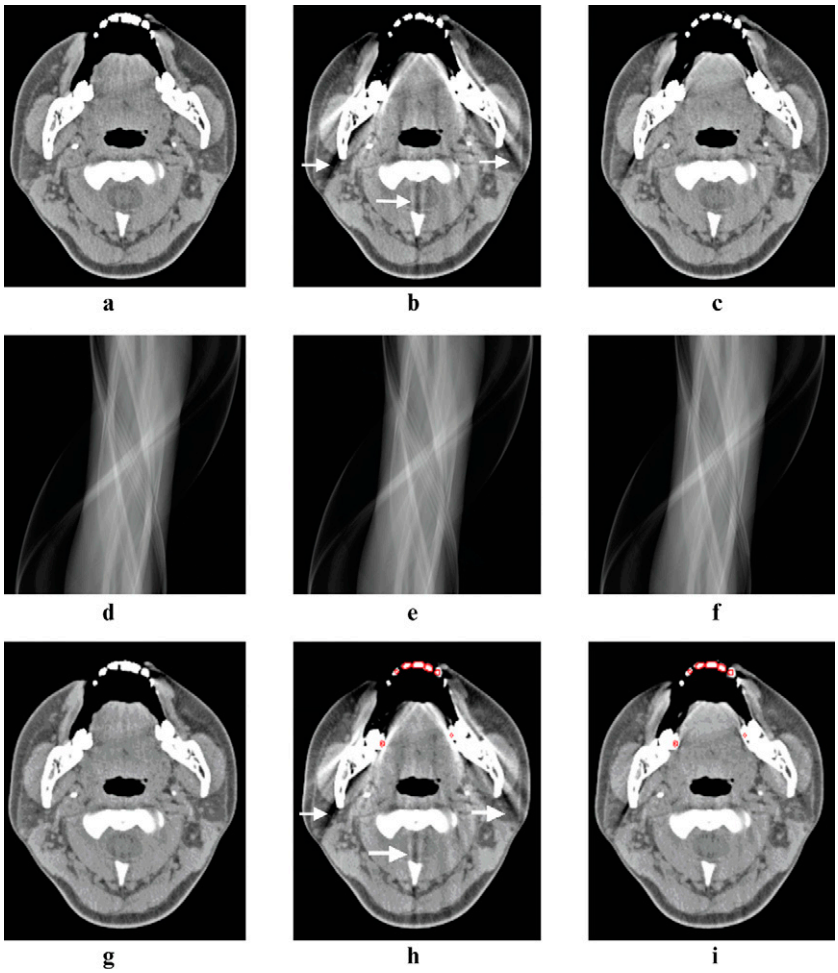

Figure 2 The image with weighted filtered back-projection (WFBP) (a, g) showed some minor artefacts in the region of the tongue and spinal canal. However, many new streak artefacts (arrows) appeared on the same image with the linear interpolation metal artefact reduction (MARli) algorithm (b) around the mandible and cervical spine. Compared with the MARli algorithm, the normalized metal artefact reduction (NMAR) algorithm (c) generated fewer new streak artefacts. (d–f) The corresponding sinograms of the WFBP, MARli and NMAR algorithms. The sinograms were created by forward-projecting from the final images after the metal artefact reduction algorithms were applied. Metal mask contours for MARli (h) and NMAR (i) are indicated on corresponding images with red circles

NMAR has the lowest mean SD value in all five ROIs, which is significantly different from WFBP (ROI_2, ROI_5 and ROI_6) and MARli (ROI_2 to ROI_6). In ROI_3 and ROI_4, the SD with MARli is even greater than the SD with WFBP (Table 2).

Discussion

Dental fillings caused severe streak artefacts and the visualization of structures close to or even distant from the metal materials deteriorated when the images were reconstructed with the WFBP algorithm. The reasons for the significant artefacts include beam hardening or photon starvation and non-linear partial volume effects due to the sharp edges of the fillings.[4,16] To correct these artefacts, effective sinogram inpainting must be achieved. The linear interpolation technique is a frequently used technique to remove metal artefacts.[16–18] In our study, the darkest streaks caused by beam hardening were significantly corrected with MARli. Nevertheless, MARli did not work well in correcting artefacts in the majority of images in this study. New streak artefacts were generated and the scores were even worse than with the WFBP algorithm in the qualitative evaluation. Dental fillings usually have highly irregular shapes and sharp edges. Also, the fillings are surrounded by the already highly dense material of the teeth, which makes interpolation in the sinogram prone to errors. MAR with linear interpolation cannot reliably reconstruct the information from within the metal trace.

Overcoming the drawbacks in pure interpolation methods, NMAR restores the traces of high-contrast objects in the metal shadow. The information on the shape of these traces is contained in the sinogram of the prior image. NMAR ensures a seamless fit of the surrogate data and recovery of traces of the objects that are contained in the prior image.[11] Our study demonstrated that NMAR can significantly reduce metal artefacts from dental fillings and avoids generating new

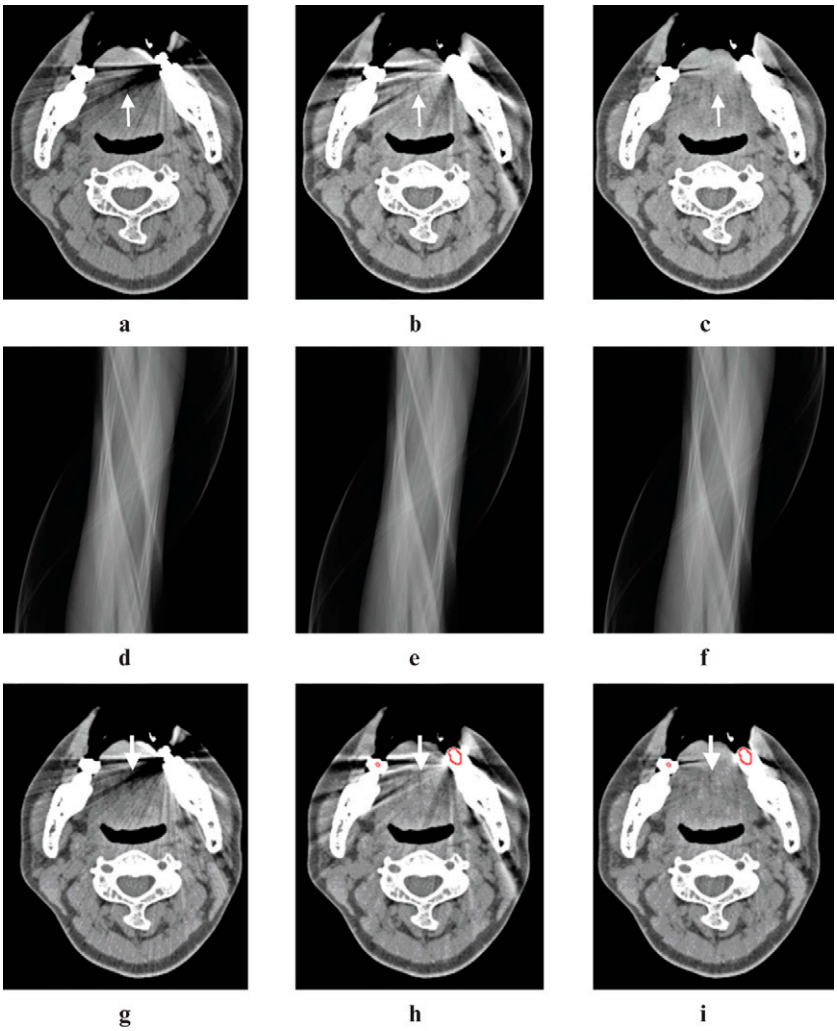

Figure 3 The image with weighted filtered back-projection (WFBP) (a, g) showed severe streak artefacts from dental fillings in the left mandible, which was evaluated as a score of 3 (arrow). Artefacts were significantly reduced with both linear interpolation metal artefact reduction (MARli) and normalized metal artefact reduction (NMAR) algorithms, with each receiving a score of 2 (arrows). The NMAR algorithm was superior to the MARli algorithm in removing the streak artefacts, especially in the region of the tongue and bilateral masseter muscles. (d–f) The corresponding sinograms of the WFBP, MARli and NMAR algorithms. The sinograms were created by forward-projecting from the final images after the metal artefact reduction algorithms were applied. Metal mask contours for MARli (h) and NMAR (i) are indicated on corresponding images with red circles

streak artefacts. NMAR has a favourable MAR result compared with the two other reconstruction techniques in qualitative evaluation.

The aim of removing dental filling artefacts was to improve the visualization of lesions in the craniofacial area that may otherwise be shadowed by the artefacts. The tongue and bilateral masseter muscles that we selected in this evaluation represented structures close to the dental fillings. A quantitative measurement showed that NMAR significantly corrected beam hardening similar to MARli. Moreover, the mean SD of CT values from soft tissues beside dental fillings was also significantly reduced with NMAR compared with the other two methods, indicating a homogeneous distribution of

Table 1 A comparison of the mean CT values in different regions of interest (ROIs)

				p-*value*		
ROI	*WFBP*	*MARli*	*NMAR*	*WFBP* vs *MARli*	*WFBP* vs *NMAR*	*MARli* vs *NMAR*
ROI_2	66.41 ± 72.44	58.05 ± 39.73	56.98 ± 34.34	0.172	0.123	0.862
ROI_3	60.03 ± 39.48	52.23 ± 46.67	53.34 ± 22.09	0.086	0.140	0.807
ROI_4	49.28 ± 23.38	49.21 ± 32.44	48.21 ± 23.09	0.983	0.752	0.769
ROI_5	59.38 ± 13.37	61.19 ± 11.77	60.48 ± 8.97	0.185	0.422	0.600
ROI_6	62.02 ± 11.00	61.04 ± 13.33	60.09 ± 10.22	0.473	0.159	0.488

MARli, linear interpolation metal artefact reduction; NMAR, normalized metal artefact reduction; WFBP, weighted filtered back-projection. Data are given as mean ± standard deviation unless otherwise indicated.

Table 2 A comparison of the standard deviations of the CT values in different regions of interest (ROIs)

				p-*value*		
ROI	*WFBP*	*MARli*	*NMAR*	*WFBP* vs *MARli*	*WFBP* vs *NMAR*	*MARli* vs *NMAR*
ROI_2	65.77 ± 61.04	63.51 ± 31.64	38.87 ± 19.04	0.642	0.000[a]	0.000[a]
ROI_3	28.51 ± 18.76	45.04 ± 26.03	24.54 ± 8.55	0.000[a]	0.087	0.000[a]
ROI_4	29.14 ± 18.07	38.95 ± 17.89	26.30 ± 11.74	0.000[a]	0.168	0.000[a]
ROI_5	18.80 ± 5.10	18.87 ± 5.77	16.97 ± 3.29	0.911	0.001[a]	0.001[a]
ROI_6	17.65 ± 3.98	16.52 ± 3.31	15.70 ± 2.69	0.005[a]	0.000[a]	0.040[a]

MARli, linear interpolation metal artefact reduction; NMAR, normalized metal artefact reduction; WFBP, weighted filtered back-projection.
Data are given as mean ± standard deviation unless otherwise indicated.
[a]Statistically significant difference.

the CT values in areas between the dental fillings and indicating the successful reduction of metal artefacts.

The muscles in the bilateral posterior cervical regions represented distant structures exposed to the streak artefacts. NMAR generated considerably fewer new streaks than MARli, but, in some cases, streaks were generated by NMAR too.

There are some minor restrictions to the present application of MARli and NMAR. The images were realized as offline reconstructions, so only a retrospective correction was possible. The MARli and NMAR reconstructions in the current implementation used the entire image information and images with large fields of view (to include the head rest). As a result, spatial resolution was slightly reduced. Compared with the WFBP algorithm, the MARli and NMAR algorithms are more time consuming, as forward-projections are needed. In this study, we did not compare the capacity of NMAR to reduce artefacts from different types of dental fillings. The limitation of data sets from different kinds of filling materials does not allow us to make further analysis. This would be an interesting topic for future study.

Conclusion

Our results showed that the NMAR algorithm can significantly reduce the artefacts caused by dental fillings and improve the clarity of the soft tissue that has been blurred by artefacts, compared with filtered back-projection and MAR with linear interpolation algorithms.

References

1. Mahnken AH, Raupach R, Wildberger JE, Jung B, Heussen N, Flohr TG, et al. A new algorithm for metal artifact reduction in computed tomography: in vitro and in vivo evaluation after total hip replacement. *Invest Radiol* 2003; **38**: 769–775.
2. Schulze R, Heil U, Gross D, Bruellmann DD, Dranischnikow E, Schwanecke U, et al. Artefacts in CBCT: a review. *Dentomaxillofac Radiol* 2011; **40**: 265–273.
3. Brown JH, Lustrin ES, Lev MH, Ogilvy CS, Taveras JM. Reduction of aneurysm clip artifacts on CT angiograms: a technical note. *AJNR Am J Neuroradiol* 1999; **20**: 694–696.
4. Yu L, Li H, Mueller J, Kofler JM, Liu X, Primak AN, et al. Metal artifact reduction from reformatted projections for hip prostheses in multislice helical computed tomography: techniques and initial clinical results. *Invest Radiol* 2009; **44**: 691–696.
5. Zhang X, Wang J, Xing L. Metal artifact reduction in x-ray computed tomography (CT) by constrained optimization. *Med Phys* 2011; **38**: 701–711.
6. Nahmias C, Lemmens C, Faul D, Carlson E, Long M, Blodgett T, et al. Does reducing CT artifacts from dental implants influence the PET interpretation in PET/CT studies of oral cancer and head and neck cancer? *J Nucl Med* 2008; **49**: 1047–1052.
7. Bazalova M, Beaulieu L, Palefsky S, Verhaegena F. Correction of CT artifacts and its influence on Monte Carlo dose calculations. *Med Phys* 2007; **34**: 2119–2132.
8. Haramati N, Staron RB, Mazel-Sperling K, Freeman K, Nickoloff EL, Barax C, et al. CT scans through metal scanning technique versus hardware composition. *Comput Med Imaging Graph* 1994; **18**: 429–434.
9. Lee MJ, Kim S, Lee SA, Song HT, Huh YM, Kim DH, et al. Overcoming artifacts from metallic orthopedic implants at high-field-strength MR imaging and multi-detector CT. *Radiographics* 2007; **27**: 791–803.
10. Bamberg F, Dierks A, Nikolaou K, Reiser MF, Becker CR, Johnson TR. Metal artifact reduction by dual energy computed tomography using monoenergetic extrapolation. *Eur Radiol* 2011; **21**: 1424–1429.
11. Nakae Y, Sakamoto K, Minamoto T, Kamakura T, Ogata Y, Matsumoto M, et al. Clinical evaluation of a newly developed method for avoiding artifacts caused by dental fillings on X-ray CT. *Radiol Phys Technol* 2008; **1**: 115–122.
12. Park WS, Kim KD, Shin HK, Lee SH. Reduction of metal artifact in three-dimensional computed tomography (3D CT) with dental impression materials. *Conf Proc IEEE Eng Med Biol Soc* 2007; **2007**: 3496–3499.
13. Meyer E, Raupach R, Lell M, Schmidt B, Kachelriess M. Normalized metal artifact reduction (NMAR) in computed tomography. *Med Phys* 2010; **37**: 5482–5493.
14. Stierstorfer K, Rauscher A, Boese J, Bruder H, Schaller S, Flohr T. Weighted FBP: a simple approximate 3D FBP algorithm for multislice spiral CT with good dose usage for arbitrary pitch. *Phys Med Biol* 2004; **49**: 2209–2218.
15. Kalender WA, Hebel R, Ebersberger J. Reduction of CT artifacts caused by metallic implants. *Radiology* 1987; **164**: 576–577.
16. Boas FE, Fleischmann D. Evaluation of two iterative techniques for reducing metal artifacts in computed tomography. *Radiology* 2011; **259**: 894–902.
17. Rinkel J, Dillon WP, Funk T, Gould R, Prevrhal S. Computed tomographic metal artifact reduction for the detection and quantitation of small features near large metallic implants: a comparison of published methods. *J Comput Assist Tomogr* 2008; **32**: 621–629.
18. Robertson DD, Yuan J, Wang G, Vannier MW. Total hip prosthesis metal-artifact suppression using iterative deblurring reconstruction. *J Comput Assist Tomogr* 1997; **21**: 293–298.